J. Fluid Mech. (1990), *vol.* 215, *pp.* 195–207
Printed in Great Britain

An easy-to-use formula for contaminant dispersion

By RONALD SMITH
Department of Mathematical Sciences, University of Technology,
Loughborough LE11 3TU, UK

(Received 12 January 1989 and in revised form 10 November 1989)

A tilted Gaussian formula is given which approximately models the concentration distribution at moderate-to-large times after discharge in steady plane parallel flows.

1. Introduction

G. I. Taylor (1953, equation (28)) derived an easy-to-use Gaussian approximation for the longitudinal concentration distribution along a parallel shear flow. For a uniform discharge in Poiseuille pipe flow, Taylor's formula for the cross-sectionally averaged concentration $\bar{c}$ is

$$\bar{c} = \frac{\bar{q}}{(2\pi\sigma^2)^{\frac{1}{2}}}\exp\left(-\frac{(x-\bar{u}t)^2}{2\sigma^2}\right), \tag{1.1a}$$

with
$$\sigma^2 = \sigma^2(0)+2(D_\infty+\bar{K})\,t, \quad D_\infty = \frac{\bar{u}^2a^2}{48\kappa}. \tag{1.1b, c}$$

Here $\bar{q}$ is the discharge per unit area, $\bar{u}$ the bulk velocity, $\sigma^2(0)$ the initial longitudinal variance, K the longitudinal diffusivity, κ the transverse diffusivity, and a the pipe radius. For other flows only the expression (1.1*c*) for the shear dispersion coefficient D_∞ needs to be changed. The dotted curve in figure 1 compares Taylor's simple approximation with the (continuous curve) numerical results obtained by Gill & Ananthakrishnan (1967, figure 5).

Aris (1956) pointed out that Taylor's work fails to account for the initial inefficiency of the shear dispersion process, while Chatwin (1970) emphasized the shortcomings as regards the skewness. Gill & Sankarasubramanian (1970) showed that the initial inefficiency could be remedied by allowing more complicated time evolution for the centroid and variance, while Smith (1987) dealt with the skewness at large times by tilting the axes. The present paper combines these ingradients to derive an improved Gaussian approximation for a weighted-average concentration $\langle c\rangle$:

$$\langle c\rangle = \frac{\bar{q}}{(2\pi\Sigma^2)^{\frac{1}{2}}}\exp\left(-\frac{(x-\bar{u}t-\langle X\rangle)^2}{2\Sigma^2}\right), \tag{1.2a}$$

with
$$\langle X\rangle = -\alpha D_\infty\{1-\exp(-\Lambda T)\}, \tag{1.2b}$$

$$\Sigma^2 = \sigma^2(0)+2(D_\infty+\bar{K})\,T-2\frac{D_\infty}{\Lambda}\{1-\exp(-\Lambda T)\}-\alpha^2D_\infty^2\{1-\exp(-\Lambda T)\}^2, \tag{1.2c}$$

$$T = t+\alpha(x-\bar{u}t). \tag{1.2d}$$

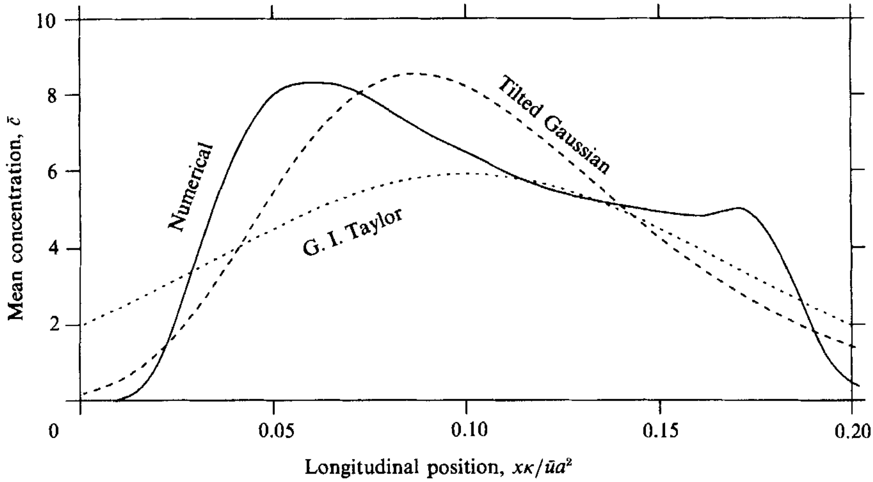

FIGURE 1. Comparison between the exact and approximate distributions in laminar pipe flow at time $0.1a^2/\kappa$ after discharge.

For Poiseuille pipe flow the shear dispersion coefficient D_∞, cross-sectional mixing rate Λ, and the skewness parameter α have the values

$$D_\infty = \frac{\bar{u}^2a^2}{48\kappa}, \quad \Lambda = \frac{100\kappa}{7a^2}, \quad \alpha = \frac{2}{5\bar{u}}. \tag{1.3a–c}$$

Tilting the axes does not change the asymptotic shear dispersion coefficient D_∞ from the value calculated by Taylor (1953). The dashed curve in figure 1 shows that this tilted Gaussian (1.2*a*–*d*) is a significant improvement upon Taylor's formula (1.1*a*–*c*), despite inevitable disparities between the different averages $\bar{c}$ and $\langle c\rangle$.

For other flows, the three parameters D_∞, Λ and α would need to be changed. The general prescription (2.3*a*–*c*) stated in the next section reveals that, if the shear dispersion coefficient D_∞ has to be calculated, then it only requires minor additional computation to evaluate the cross-sectional mixing rate Λ and the skewness parameter α. So, the claim made in the title of this paper is that the tilted Gaussian (1.2*a*–*d*) is an easy-to-use formula.

The usefulness of the formula (1.2*a*–*d*) lies in its efficacy. Hence precedence is given to illustrative examples. A derivation is deferred until the second half of this paper.

2. Statement of results

As in the now classical work of G. I. Taylor (1953), the principal task is to determine the (steady) centroid displacement function $g_0(y)$:

$$-\partial_y(m\kappa\,\partial_y g_0) = m(u-\bar{u}), \tag{2.1a}$$

$$m\kappa\,\partial_y g_0 = 0 \quad \text{on} \quad y = 0, a, \tag{2.1b}$$

and

$$\bar{g}_0 = 0. \tag{2.1c}$$

Here $m(y)$ is a transverse metric coefficient, $\kappa(y)$ the transverse diffusivity, $u(y)$ the velocity profile, and overbars denote cross-sectional averaging:

$$A = \int_0^a m\,\mathrm{d}y, \quad \bar{u} = \frac{1}{A}\int_0^a mu\,\mathrm{d}y. \tag{2.2a, b}$$

Different choices of $m(y)$ permit y to be a Cartesian or polar coordinate. For vertically well-mixed channels the same equations apply, but with $m = h$ being the water depth.

The shear dispersion coefficient D_∞, skewness parameter α, and cross-section mixing rate Λ merely involve integrals of g_0:

$$D_\infty = \overline{(u-\bar{u})\,g_0}, \quad \alpha = \frac{\overline{(u-\bar{u})\,g_0^2}}{2D_\infty^2}, \tag{2.3a, b}$$

$$\Lambda = \frac{D_\infty}{\overline{g_0^2}+\alpha^2 D_\infty^2}. \tag{2.3c}$$

To calculate the weighted average concentration $\langle c\rangle$, we employ these three parameters D_∞, α, Λ in the tilted Gaussian formula (1.2*a–d*).

If we are more ambitious and seek the y-structure of the concentration field $c(x, y, t)$, then we use another tilted Gaussian:

$$c = \frac{\bar{q}}{(2\pi\langle\sigma^2\rangle)^{\frac{1}{2}}}\exp\left(-\frac{(x-\bar{u}t-X)^2}{2\langle\sigma^2\rangle}\right), \tag{2.4a}$$

with
$$X(y,t) = \{g_0(y)-\alpha D_\infty\}\{1-\exp(-\Lambda T)\}, \tag{2.4b}$$

$$\langle\sigma^2\rangle = \sigma^2(0)+2(D_\infty+\bar{K})\,T-\frac{3D_\infty}{\Lambda}+\frac{4D_\infty}{\Lambda}\exp(-\Lambda T)-\frac{D_\infty}{\Lambda}\exp(-2\Lambda T), \tag{2.4c}$$

$$T = t+\alpha(x-\bar{u}t). \tag{2.4d}$$

Here $\sigma^2(0)$ is the initial variance of the discharge and $K(y)$ is the longitudinal diffusivity.

The above formulae (1.2*a–d*), (2.4*a–d*) only apply to uniform discharges. For a non-uniform discharge $q(y)$, the Gaussian approximation for $\langle c\rangle$ needs to be modified:

$$\langle c\rangle = \frac{\bar{q}}{(2\pi\Sigma^2)^{\frac{1}{2}}}\exp\left(-\frac{(x-\bar{u}t-\langle\phi X\rangle)^2}{2\Sigma^2}\right), \tag{2.5a}$$

with
$$\langle\phi X\rangle = \left\{\frac{\overline{g_0\,q}}{\bar{q}}-\alpha D_\infty\right\}\{1-\exp(-\Lambda T)\}, \tag{2.5b}$$

$$\Sigma^2 = \sigma^2(0)+2(D_\infty+\bar{K})\,T-2\frac{D_\infty}{\Lambda}\{1-\exp(-\Lambda T)\}$$
$$+2\left\{\frac{\overline{g_0^2 q}}{\bar{q}}-\overline{g_0^2}-2\alpha D_\infty\frac{\overline{g_0 q}}{\bar{q}}\right\}\{1-(1+\Lambda T)\exp(-\Lambda T)\}-\langle\phi X\rangle^2. \tag{2.5c}$$

3. Poiseuille pipe flow

In applying the above prescription to laminar pipe flow, we write

$$r = y, \quad m = r, \quad \kappa = \text{constant}, \quad u = 2\bar{u}(1-(r/a)^2). \tag{3.1a–d}$$

The (conventional) centroid displacement function is given by

$$g_0 = \frac{\bar{u}a^2}{24\kappa}\{2-6(r/a)^2+3(r/a)^4\}. \tag{3.2}$$

The requisite integrals of g_0 have the values

$$\overline{(u-\bar{u})\,g_0} = \frac{\bar{u}^2a^2}{48\kappa},\quad \overline{(u-\bar{u})\,g_0^2} = \frac{\bar{u}^3a^4}{2880\kappa^2},\quad \overline{g_0^2} = \frac{\bar{u}^2a^4}{720\kappa^2}. \tag{3.3a–c}$$

The general formulae (2.3*a–c*) for D_∞, α and Λ yield the results already used in the introduction:

$$D_\infty = \frac{\bar{u}^2a^2}{48\kappa},\quad \alpha = \frac{2}{5\bar{u}},\quad \Lambda = \frac{100\kappa}{7a^2}. \tag{3.4a–c}$$

The results shown in figure 1 correspond to a moderate value of the non-dimensional time since discharge

$$\Lambda t = 1.428. \tag{3.5}$$

So, it is to be expected that large-time approximations, such as derived by Taylor (1953), are not very accurate. Alas, the tilted Gaussian does not reproduce the small-time feature of the forwards peak associated with high concentrations carried along at nearly the peak velocity $2\bar{u}$ in the fluid close to the centre of the pipe.

4. Plane Poiseuille flow

For laminar flow between parallel plates $2a$ apart, we have

$$m = 1,\quad \kappa = \text{constant},\quad u = \tfrac{3}{2}\bar{u}(1-(y/a)^2). \tag{4.1a–c}$$

The (conventional) centroid displacement function is

$$g_0 = \frac{\bar{u}a^2}{120\kappa}\{7-30(y/a)^2+15(y/a)^4\}. \tag{4.2}$$

The necessary integrals of g_0 are

$$\overline{(u-\bar{u})\,g_0} = \frac{2\bar{u}^2a^2}{105\kappa},\quad \overline{(u-\bar{u})\,g_0^2} = -\frac{4\bar{u}^3a^4}{17\,325\kappa^2},\quad \overline{g_0^2} = \frac{\bar{u}^2a^4}{525\kappa^2}. \tag{4.3a–c}$$

The general formulae (2.3*a–c*) for D_∞, α and Λ yield the results

$$D_\infty = \frac{2\bar{u}^2a^2}{105\kappa},\quad \alpha = \frac{-7}{22\bar{u}},\quad \Lambda = \frac{363\kappa}{37a^2}. \tag{4.4a–c}$$

Jayaraj & Subramanian (1978, figure 2) give numerical results for the concentration contours after a time lapse

$$t = 0.1\frac{a^2}{\kappa},\quad \Lambda t = 0.98. \tag{4.5a, b}$$

These are shown by the continuous curves in figure 2. The tilted Gaussian (2.4*a–d*) yields the dashed contours. Although the overall agreement is reasonable, the approximation fails to indicate any secondary concentration maxima at the channel walls.

Figure 3 gives the corresponding comparisons between the numerical solution for $\bar{c}$ (Jayaraj & Subramanian 1978, figure 3) and tilted Gaussian approximation (1.2*a–d*) for $\langle c\rangle$. For completeness we include the dotted curve which shows the

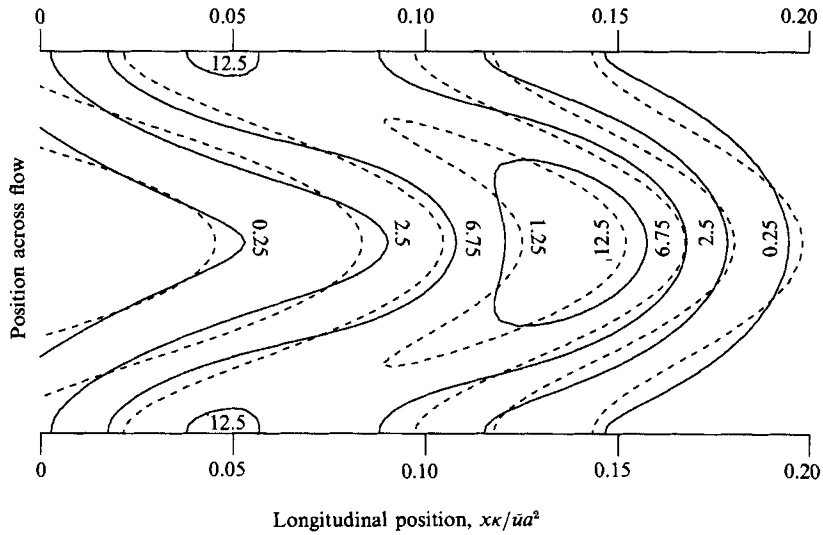

FIGURE 2. Comparison between the exact (——) and tilted Gaussian (---) concentration contours in plane Poiseuille flow at time $0.1a^2/\kappa$ after discharge.

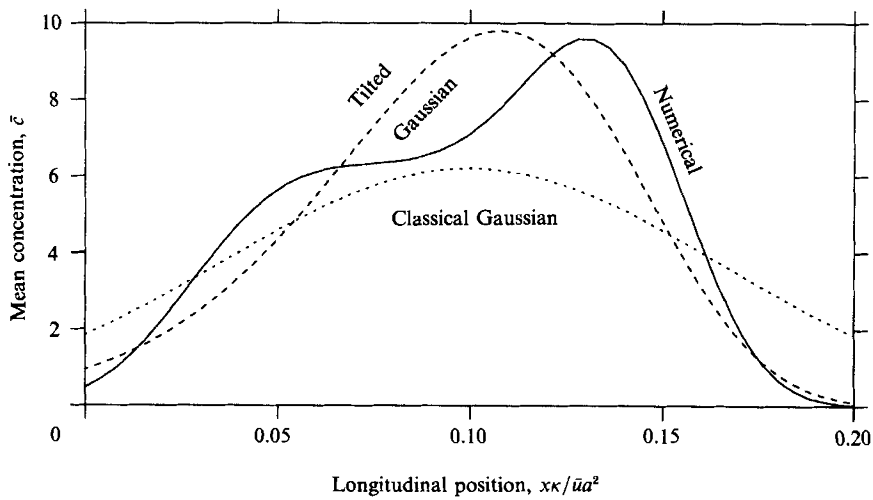

FIGURE 3. Comparison between the exact and approximate distributions for the cross-sectionally averaged concentration $\bar{c}$ in plane Poiseuille flow at time $0.1a^2/\kappa$ after discharge.

classical Gaussian prediction for $\bar{c}$ (equation (1.1*a*)) with no allowance for skewness nor memory. Again, the main shortcoming of the tilted Gaussian is that it does not reproduce the small-time feature of the secondary peak.

5. Two-layer flows

For two well-mixed layers of velocities u_+, u_- and fractional areas a_+, a_- with an e-folding rate λ for mixing between the layers, the (conventional) centroid displacement function can be written

$$g_+ = \frac{a_-}{\lambda}(u_+ - u_-), \quad g_- = \frac{-a_+}{\lambda}(u_+ - u_-). \tag{5.1a, b}$$

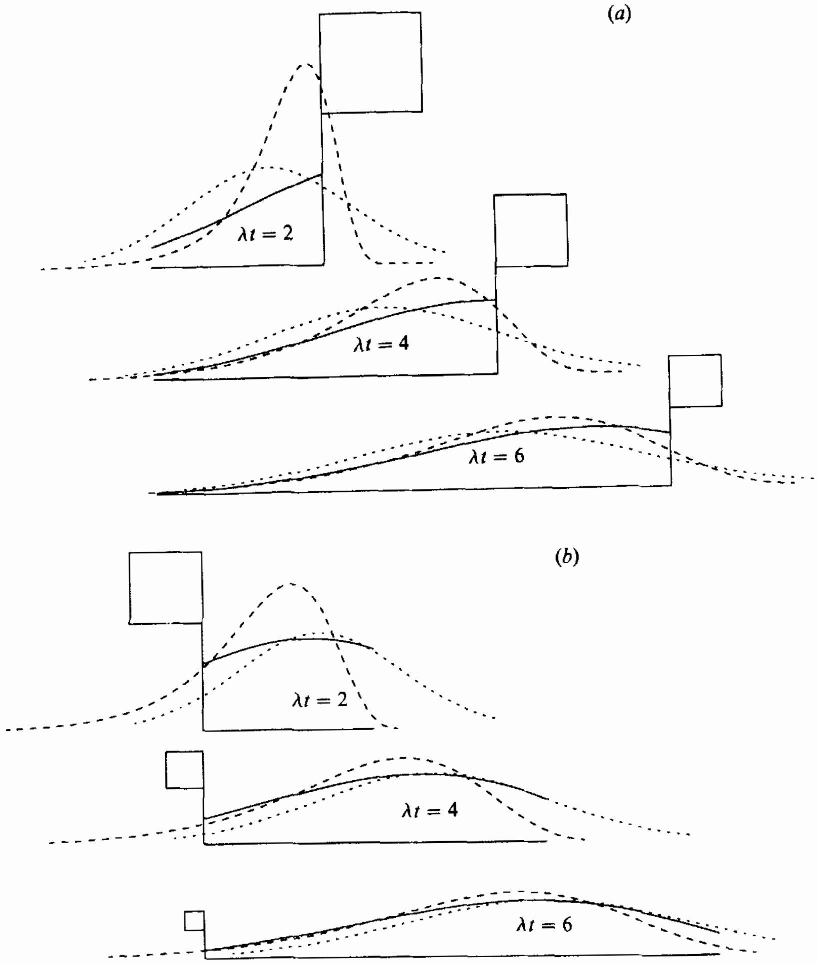

FIGURE 4. Comparison between the exact (——) solution for $\bar{c}$, the conventional Gaussian (......) for $\bar{c}$, and tilted Gaussian (-----) for $\langle c \rangle$ in a two-layer flow when the discharge is confined to (*a*) the faster layer, (*b*) the slower layer. The area under the delta-function spikes in the exact solution is indicated by the area of the flags.

The + subscripts refer to the faster-moving layer. Where previously we had to evaluate integrals (2.3*a*–*c*), we now just have two-term summations:

$$D_\infty = \frac{a_+ a_-}{\lambda}(u_+ - u_-)^2, \quad \alpha = \frac{-(a_+ - a_-)}{2a_+ a_-(u_+ - u_-)}, \tag{5.2a, b}$$

$$\Lambda = 4a_+ a_- \lambda. \tag{5.2c}$$

Thacker (1976) gave the exact solution for equal layers, which Smith (1981, §5) generalized to unequal layers. For a sudden discharge q_+, q_- at $x = 0, t = 0$ the exact solution for $\bar{c}(x,t)$ has delta-function spikes at the end points:

$$\bar{c} = a_- q_- \delta(x - u_- t) \exp(-a_+ \lambda t), \tag{5.3a}$$

$$\bar{c} = a_+ q_+ \delta(x - u_- t) \exp(-a_- \lambda t), \tag{5.3b}$$

with a modified Bessel function representation in the central region $u_- t < x < u_+ t$:

$$\bar{c} = \frac{2a_+ a_- \lambda}{u_+ - u_-}\left\{\tfrac{1}{2}(q_+ + q_-) I_0(r) + \frac{\lambda}{u_+ - u_-}(a_+ q_+(x - u_- t) + a_- q_-(u_+ t - x))\frac{I_1(r)}{r}\right\}$$

$$\times \exp\left\{-\frac{\lambda}{u_+ - u_-}(a_-(x - u_- t) + a_+(u_+ t - x))\right\}, \quad (5.3c)$$

where

$$r^2 = \frac{4\lambda^2 a_+ a_-}{(u_+ - u_-)^2}(x - u_- t)(u_+ t - x). \quad (5.3d)$$

Figure 4 (a) compares the exact and conventional Gaussian solutions for $\bar{c}(x,t)$ with the tilted Gaussian for $\langle c \rangle$ when the discharge is confined to the faster layer in the dead-zone case

$$u_- = 0, \quad u_+ = 1.5\bar{u} \quad (a_- = \tfrac{1}{3}, \quad a_+ = \tfrac{2}{3}). \quad (5.4)$$

Figure 4 (b) gives the comparisons in the opposite extreme of a discharge confined to the slower layer. Although the finite propagation speeds and the concentration spikes are not modelled, for small values of λt the tilted Gaussian is a significant improvement upon the classical Gaussian approximation.

6. Starting point for the derivation

For a high-Péclet-number, parallel shear flow in the x-direction, the advection–diffusion equation takes the form

$$m\,\partial_t c + mu\,\partial_x c - \partial_y(m\kappa\,\partial_y c) = 0, \quad (6.1a)$$

with

$$m\kappa\,\partial_y c = 0 \quad \text{on} \quad y = 0, a, \quad (6.1b)$$

and

$$c = q(y)\,\delta(x) \quad \text{at} \quad t = 0. \quad (6.1c)$$

For simplicity it has been assumed that the discharge is of negligible longitudinal or temporal extent. Also, we have ignored any longitudinal diffusion $K\,\partial_x^2 c$, on the basis that the Péclet number ua/κ is large and velocity effects soon dominate diffusion.

Some of these approximations can be rectified easily. For example, Aris (1956) showed that longitudinal diffusion $K(y)$ increases the shear dispersion coefficient by $\bar{K}$. Similarly, if the initial discharge has variance $\sigma^2(0)$ then the variance needs to be augmented by this amount. These minor corrections have been included in the results stated in §§1 and 2, and have a small but perceptible improving effect on the performance of the new Gaussian approximations in figures 1–4.

If we use a tilted evolutionary coordinate

$$T = t + \alpha(x - \bar{u}t), \quad (6.2)$$

then the field equation satisfied by $c(x, y, t)$ takes the modified form

$$m\{1 + \alpha(u - \bar{u})\}\,\partial_T c + mu\,\partial_x c - \partial_y(m\kappa\,\partial_y c) = 0. \quad (6.3)$$

The initial condition is also modified slightly:

$$\{1 + \alpha(u - \bar{u})\}\,c = q(y)\,\delta(x) \quad \text{at} \quad T = 0. \quad (6.4)$$

7. Building-in prior knowledge

To make our approximations as efficient as possible, we try to exploit our prior knowledge of what to expect. For example, Aris (1956) showed that at large times after discharge the contaminant cloud will be carried along at the bulk velocity $\bar{u}$, but with a displacement between the centroid position at different levels across the flow. Also, the marked skewness at large times after discharge can be suppressed by the use of tilted axes (Smith 1987). Thus, we define a coordinate system

$$\xi = x - \bar{u}t - X(y, T), \tag{7.1a}$$

$$T = t + \alpha(x - \bar{u}t), \tag{7.1b}$$

where the centroid displacement function $X(y, T)$ is defined below in (7.6*a–c*).

To a first approximation the cross-stream concentration profile $\phi(y, T)$ is related to the discharge shape $q(y)$:

$$m\{1+\alpha(u-\bar{u})\}\,\partial_T\phi - \partial_y(m\kappa\,\partial_y\phi) = 0, \tag{7.2a}$$

with $$m\kappa\,\partial_y\phi = 0 \quad \text{on} \quad y = 0, a, \tag{7.2b}$$

and $$\{1+\alpha(u-\bar{u})\}\,\phi = q(y)/\bar{q} \quad \text{at} \quad T = 0. \tag{7.2c}$$

We remark that ϕ is non-negative and satisfies the normalization

$$\langle\phi\rangle = 1, \tag{7.3}$$

where the angle brackets denote a weighted average:

$$\langle c\rangle = \frac{1}{A}\int_0^a \{1+\alpha(u-\bar{u})\}\,cm\,\mathrm{d}y. \tag{7.4}$$

At large times after discharge $\phi(y, T)$ becomes uniform:

$$\phi(y, T) \sim 1. \tag{7.5}$$

The centroid displacement $X(y, T)$ satisfies the transverse diffusion equation

$$m\{1+\alpha(u-\bar{u})\}\,\partial_T(\phi X) - \partial_y(m\kappa\,\partial_y(\phi X)) = m(u-\bar{u})\,\phi, \tag{7.6a}$$

with $$m\kappa\,\partial_y(\phi X) = 0 \quad \text{on} \quad y = 0, a, \tag{7.6b}$$

and $$\phi X = 0 \quad \text{at} \quad T = 0. \tag{7.6c}$$

The evolution of $\langle\phi X\rangle$ is related to that of ϕ:

$$\langle\phi X\rangle = \frac{\overline{g_0 q}}{\bar{q}} - \langle g_0\phi\rangle, \tag{7.7}$$

where $g_0(y)$ is the (steady) centroid displacement function as defined in (2.1*a–c*). At large times we can infer that the y-dependence of ϕX is the same as that of $g_0(y)$:

$$\phi X - \overline{\phi X} \sim g_0(y) \quad \text{or} \quad \phi X - \langle\phi X\rangle \sim g_\infty(y), \tag{7.8a, b}$$

where $$g_\infty(y) = g_0(y) - \alpha D_\infty, \quad \langle g_\infty\rangle = 0. \tag{7.8c, d}$$

Together, (7.7), (7.8*b*) yield the asymptote

$$X \sim g_\infty(y) + \frac{\overline{g_\infty q}}{\bar{q}}. \tag{7.9}$$

In the tilted, centroid-following coordinate system we replace the advection–diffusion equation (6.1) by

$$m\{1+\alpha(u-\bar{u})\}\partial_T c+2m\kappa\,\partial_y X\left(\partial_y\partial_\xi c\frac{-\partial_y\phi}{\phi}\partial_\xi c\right)-m\kappa(\partial_y X)^2\partial_\xi^2 c-\partial_y(m\kappa\,\partial_y c)=0, \tag{7.10a}$$

with $$m\kappa\,\partial_y c=0 \quad \text{on} \quad y=0,a, \tag{7.10b}$$

and $$\{1+\alpha(u-\bar{u})\}c=q(y)\,\delta(\xi) \quad \text{at} \quad T=0. \tag{7.10c}$$

So much information has been built-in to these equations (via ϕ and X) that it is now only a simple task to derive a diffusion approximation.

8. Diffusion approximation

We decompose $c(\xi,y,T)$ into a part associated with $\phi(y,T)$ and a perturbation c':

$$c=\langle c\rangle\phi+c' \quad \text{with} \quad \langle c'\rangle=0. \tag{8.1a, b}$$

The cross-sectionally averaged version of (7.10a) is

$$\partial_T\langle c\rangle-\overline{\kappa\phi(\partial_y X)^2}\,\partial_\xi^2\langle c\rangle+2\,\partial_\xi\overline{\kappa\phi\,\partial_y X\,\partial_y(c'/\phi)}-\partial_\xi^2\,\overline{\kappa(\partial_y X)^2 c'}=0. \tag{8.2}$$

A diffusion model (Taylor 1953) for the evolution of $\langle c\rangle$ merely requires the total neglect of c':

$$\partial_T\langle c\rangle-D\,\partial_\xi^2\langle c\rangle=0, \tag{8.3a}$$

with $$D(T)=\overline{\kappa\phi(\partial_y X)^2}=\overline{(u-\bar{u})\,\phi X}-\tfrac{1}{2}\partial_T\langle\phi X^2\rangle. \tag{8.3b}$$

At large times $X(y,T)$ becomes steady, and the asymptotic value of the shear dispersion coefficient $D(T)$ conforms precisely with the value D_∞ calculated by Taylor (1953):

$$D_\infty=\overline{(u-\bar{u})\,g_0}. \tag{8.4}$$

At earlier times the non-negative character of $D(T)$ is a simple consequence of the non-negative character of ϕ.

For a sudden discharge at $T=\xi=0$ the solution of (8.3a) is a Gaussian distribution for $\langle c\rangle$:

$$\langle c\rangle=\frac{\bar{q}}{(2\pi\langle\phi\sigma^2\rangle)^{\frac{1}{2}}}\exp\left(-\frac{\xi^2}{2\langle\phi\sigma^2\rangle}\right), \tag{8.5a}$$

with $$\langle\phi\sigma^2\rangle=2\int_0^T D(T')\,\mathrm{d}T',$$

$$=2\int_0^T\overline{(u-\bar{u})\,\phi X}\,\mathrm{d}T'-\langle\phi X^2\rangle. \tag{8.5b}$$

If we reinstate the $\phi(y,T)$ factor, but neglect c', then this is a tilted Gaussian approximation for the y-dependent concentration distribution $c(x,y,t)$. The Gaussian (2.4a–d) corresponds to the elementary case in which $\phi=1$.

It deserves emphasis that the Gaussian (8.5a, b) is a solution of the model equation (8.3) and not of the full equation (8.2). For non-optimal α the dominant error is associated with the skewness and decays at the slow rate $T^{-\frac{1}{2}}$ (Chatwin 1970). For optimal α the dominant error is associated with the kurtosis (spikiness) and decays at the rate T^{-1}. Indeed, the two-humped profiles shown in figures 1, 3 and the delta-function spikes in figure 4(a, b) are extreme examples of the spikiness and non-Gaussianity at short times after discharge.

9. A Gaussian for $\langle c\rangle$

The definition (7.1a) of the centroid-following coordinate ξ, allows us to rewrite the Gaussian (8.5a):

$$c=\frac{\bar{q}\phi}{(2\pi\langle\phi\sigma^2\rangle)^{\frac{1}{2}}}\exp\left(-\frac{(x-\bar{u}t-X(y,T))^2}{2\langle\phi\sigma^2\rangle}\right)+c'. \tag{9.1}$$

The usual requirement is an approximation in the conventional x, y coordinates for the cross-sectionally averaged concentration $\bar{c}$. To do this would require some knowledge of the error term c'. So instead we derive an approximation for $\langle c\rangle$.

Following Smith (1987, §7), we make the definitions

$$\Sigma^2=\langle\phi\sigma^2\rangle+\langle\phi(X-\langle\phi X\rangle)^2\rangle,\quad \zeta=\frac{x-\bar{u}t-\langle\phi X\rangle}{\Sigma}. \tag{9.2a, b}$$

For large Σ^2 the Gaussian (9.1) can be expanded as a Hermite series:

$$\frac{\bar{q}\phi}{(2\pi\Sigma^2)^{\frac{1}{2}}}\exp(-\tfrac{1}{2}\zeta^2)\left\{1+\frac{X-\langle\phi X\rangle}{\Sigma}\mathrm{He}_1(\zeta)+\frac{(X-\langle\phi X\rangle)^2-\langle(\phi X-\langle\phi X\rangle)^2\rangle}{2\Sigma^2}\mathrm{He}_2(\zeta)\right.$$
$$\left.+\frac{(X-\langle\phi X\rangle)^3}{6\Sigma^3}\mathrm{He}_3(\zeta)+\ldots\right\}. \tag{9.3}$$

By construction the coefficients of He_1 and He_2 have zero weighted average values. Hence, we pose the Gaussian approximation

$$\langle c\rangle=\frac{\bar{q}}{(2\pi\Sigma^2)^{\frac{1}{2}}}\exp\left(-\frac{(x-\bar{u}t-\langle\phi X\rangle)^2}{2\Sigma^2}\right), \tag{9.4a}$$

with

$$\Sigma^2=2\int_0^T\overline{(u-\bar{u})\phi X}\,\mathrm{d}T'-\langle\phi X\rangle^2. \tag{9.4b}$$

By not resolving the y-dependent centroid displacement $X(y,t)$, we pay the price of an increased variance Σ^2 instead of $\langle\phi\sigma^2\rangle$. The neglected He_3 term decays as T^{-3} and is much smaller than the intrinsic error in the original formula (8.5a) (Chatwin 1970).

For a uniform discharge and with $\alpha=0$ the time-dependence of Σ^2 is identical to that yielded by the work of Gill & Sankarasubramanian (1970, equations 10a, 14). Indeed, although (9.1), (9.4a) are approximations, it happens that the area and centroid are exact. If $\phi=1$ then the variance is also exact. The neglected terms only influence the skewness, kurtosis, ... Hence, as in the work of Gill & Sankarasubramanian (1970), the predictions will be credible even at small times when the departures c' from the ϕ-profile may be large.

10. One-mode model

The exact solution for $\phi(y,T)$ can be given in terms of eigenmodes ψ_n and eigenvalues λ_n:

$$\partial_y(m\kappa\,\partial_y\psi_n)+\lambda_n m\{1+\alpha(u-\bar{u})\}\psi_n=0, \tag{10.1a}$$

with $$m\kappa\,\partial_y \psi_n = 0 \quad \text{on} \quad y = 0, a, \tag{10.1b}$$

and $$\langle \psi_n^2 \rangle = 1. \tag{10.1c}$$

The lowest mode is uniform and non-decaying

$$\psi_0 = 1, \quad \lambda_0 = 0. \tag{10.2a, b}$$

The solution for $\phi(y, T)$ is

$$\phi = 1 + \sum_{n=1}^{\infty} \frac{\overline{q\psi_n}}{\bar{q}} \psi_n(y) \exp(-\lambda_n T). \tag{10.3}$$

To represent the right-hand-side forcing terms in (7.6*a*) we introduce the velocity coefficients

$$u_{mn} = \overline{(u - \bar{u})\,\psi_m \psi_n}. \tag{10.4}$$

As the mode numbers m, n increase the modes ψ_m, ψ_n become increasingly oscillatory and the coefficients u_{mn} become small. The exact solution for ϕX is

$$\phi X = \sum_{n=1}^{\infty} \left(\frac{\overline{q\psi_n}}{\bar{q}} + \psi_n(y) \right) \frac{u_{n0}}{\lambda_n} \{1 - \exp(-\lambda_n T)\}$$
$$+ \sum_{n=1}^{\infty} \frac{\overline{q\psi_n}}{\bar{q}} \psi_n(y)\, u_{nn}\, T \exp(-\lambda_n T) + \sum_{n=1}^{\infty} \sum_{\substack{m=1 \\ m \neq n}}^{\infty} u_{mn} \frac{\overline{q\psi_m}}{\bar{q}} \psi_n(y)\, J_{mn}(T), \tag{10.5a}$$

where $$J_{mn}(T) = \frac{\exp(-\lambda_m T) - \exp(-\lambda_n T)}{\lambda_n - \lambda_m}. \tag{10.5b}$$

From the large-T asymptote (7.9) we can infer that

$$g_\infty(y) = \sum_{n=1}^{\infty} \frac{u_n}{\lambda_n} \psi_n(y), \tag{10.6a}$$

$$D_\infty = \sum_{n=1}^{\infty} \frac{u_{n0}^2}{\lambda_n}, \quad \langle g_\infty^2 \rangle = \sum_{n=1}^{\infty} \frac{u_{n0}^2}{\lambda_n^2}. \tag{10.6b, c}$$

It is easy to calculate $g_\infty(y)$ but difficult to calculate the eigenmodes ψ_n and eigenvalues λ_n. So, we merely use the exact solutions (10.3), (10.5) as guides in our selection of one-mode approximations. In particular, if the series (10.6*a*–*c*) converge rapidly, then the leading non-uniform mode can be approximated:

$$\Psi(y) = \frac{g_\infty(y)}{\langle g_\infty^2 \rangle^{\frac{1}{2}}}, \quad \Lambda = \frac{D_\infty}{\langle g_\infty^2 \rangle} \tag{10.7a, b}$$

(Smith 1981).

Formulae for ϕ and for ϕX which have the correct symmetry between the q- and y-dependence, and are exact in the one-mode limit, are

$$\phi = 1 + \frac{\overline{q g_\infty}\, g_\infty(y)}{\bar{q} \langle g_\infty^2 \rangle} \exp(-\Lambda T), \tag{10.8a}$$

$$\phi X = \left(\frac{\overline{q g_\infty}}{\bar{q}} + g_\infty(y) \right) \{1 - \exp(-\Lambda T)\}$$
$$+ \left(\left(\frac{g_\infty^2}{\langle g_\infty^2 \rangle} - 1 \right) \frac{q}{\bar{q}} g_\infty(y) + \frac{\overline{g_\infty q}}{\bar{q}} \left(\frac{g_\infty^2}{\langle g_\infty^2 \rangle} - 1 \right) - \frac{\overline{g_\infty q}\, g_\infty(y)\, \overline{(u - \bar{u})\, g_\infty^2}}{\bar{q} \langle g_\infty^2 \rangle\, \overline{(u - \bar{u})\, g_\infty}} \right) \Lambda T \exp(-\Lambda T). \tag{10.8b}$$

The corresponding one-mode approximations for $\langle \phi X \rangle$ and for Σ^2 are

$$\langle \phi X \rangle = \frac{\overline{q g_\infty}}{\bar{q}} \{1 - \exp(-\Lambda T)\}, \tag{10.9a}$$

$$\Sigma^2 = 2D_\infty T - 2\frac{D_\infty}{\Lambda}\{1 - \exp(-\Lambda T)\}$$
$$+ \overline{\left(\frac{g_\infty^2}{\langle g_\infty^2 \rangle} - 1\right)\frac{q}{\bar{q}}} \, 2\frac{D_\infty}{\Lambda}\{1 - (1 + \Lambda T)\exp(-\Lambda T)\} - \langle \phi X \rangle^2. \tag{10.9b}$$

For a uniform discharge and with $\alpha = 0$, the accuracy of such one-mode approximations for Σ^2 has been tested by Smith (1981, figures 2, 5, 8). To recover the formulae (2.5*b*, *c*) given in the statement of results, we include the allowance for the initial variance $\sigma^2(0)$ and for the longitudinal diffusivity $K(y)$.

The non-negative property of $\phi(y, T)$ is lost in the truncation (10.8*a*). It is for that reason that the y-dependent Gaussian (2.4*a*) should strictly be restricted to the case in which $\phi = 1$. Fortunately, the formulae (10.9*b*) for Σ^2 does remain positive for all discharge profiles $q(y)$. So the formula (2.5*a*) is applicable at all times, even though its accuracy may be poor for small ΛT when higher modes might not have decayed away. The leading term for small ΛT is

$$\Sigma^2 \sim \Lambda^2 T^2 \overline{\left(g_\infty - \frac{\overline{g_\infty q}}{\bar{q}}\right)^2 \frac{q}{\bar{q}}}. \tag{10.10}$$

The spatial error in the tilted Gaussian (2.4) can be explained in terms of the modes. The $g_0(y)$- and Λ-terms account for the longest-persisting $\psi_1(y)$ mode. However, the next longest-persisting mode $\psi_2(y)$ is not accommodated. In figure 2 the concentration maxima along the boundary and along the centreline are both under-predicted, while at intermediate y-positions the concentration maxima are over-predicted. In the concentration tails the signs of the errors are reversed: along the boundary and along the centreline the concentrations are over-predicted, with under-prediction at intermediate positions.

It is by accounting for the ψ_1 mode that the tilted Gaussians (2.4), (2.5) become useful earlier than the classical Gaussian (1.1). The test cases shown in figures 1, 3 are flattering to the classical Gaussian, because the centroid position happens to be correct for a uniform discharge. So, the greater accuracies of the tilted Gaussians in figures 1, 3 are attributable to the ψ_1-related modifications to the variance. The subsequent decay of the errors is as $(\Lambda t)^{-1}$, which is faster than the classical rate $(\Lambda t)^{-\frac{1}{2}}$ (Chatwin 1970).

11. Choosing the skewness parameter

When we ceased to resolve the y-dependence of the centroid displacement $X(y, T)$, the associated blurring of the concentration distribution resulted in an increase of variance from $\langle \phi \sigma^2 \rangle$ to Σ^2. Similarly, we can expect that an inappropriate choice of tilted axes would increase both $\langle \sigma^2 \rangle$ and Σ^2. Accordingly, we seek to maximize $\langle g_\infty^2 \rangle$, or minimize Λ (see (10.7*b*) and (10.9*b*)).

To highlight the α-dependence, we write

$$\langle g_\infty^2 \rangle = \overline{g_0^2} + \alpha\overline{(u - \bar{u})\, g_0^2} - \alpha^2 D_\infty^2. \tag{11.1}$$

This attains its maximum with respect to α at

$$\alpha = \frac{\overline{(u-\bar{u})\, g_0^2}}{2D_\infty^2}. \tag{11.2}$$

Reassuringly, this is precisely the value of the skewness parameter α which minimizes the eventual skewness (Smith 1987, equation (4.8)). With this particular value of α, the formula (10.7*b*) for A can be written as given in the statement of results:

$$A = \frac{D_\infty}{g_0^2 + \alpha^2 D_\infty^2}. \tag{11.3}$$

At this stage the derivation is complete. For the method of application and tests of accuracy we refer back to the first five sections of this paper.

I wish to thank the Royal Society for financial support.

REFERENCES

Aris, R. 1956 On the dispersion of a solute in a fluid flowing through a tube. *Proc. R. Soc. Lond.* A **235**, 67–77.

Chatwin, P. C. 1970 The approach to normality of the concentration distribution of a solute in solvent flowing along a straight pipe. *J. Fluid Mech.* **43**, 321–352.

Gill, W. N. & Ananthakrishnan, V. 1967 Laminar dispersion in capillaries. Part 4. The slug stimulus. *AIChE J.* **13**, 801–807.

Gill, W. N. & Sankarasubramanian, R. 1970 Exact analysis of unsteady convective diffusion. *Proc. R. Soc. Lond.* A **316**, 341–350.

Jayaraj, K. & Subramanian, R. S. 1978 On relaxation phenomena in field-flow fractionation. *Sep. Sci. Tech.* **13**, 791–817.

Smith, R. 1981 A delay-diffusion description for contaminant dispersion. *J. Fluid Mech.* **105**, 469–486.

Smith, R. 1987 Shear dispersion looked at from a new angle. *J. Fluid Mech.* **182**, 447–466.

Taylor, G. I. 1953 Dispersion of soluble matter in solvent flowing slowly through a tube. *Proc. R. Soc. Lond.* A **219**, 186–203.

Thacker, W. C. 1976 A solvable model of shear dispersion. *J. Phys. Oceanogr.* **6**, 66–75.